Load- and displacement-controlled finite element analyses on fusion and non-fusion spinal implants

Z-C Zhong, S-H Chen and C-H Hung

Proceedings of the Institution of Mechanical Engineers, Part H: Journal of Engineering in Medicine 2009 223: 143
DOI: 10.1243/09544119JEIM476

Load- and displacement-controlled finite element analyses on fusion and non-fusion spinal implants

Z-C Zhong[1], **S-H Chen**[2], and **C-H Hung**[1]*
[1]Department of Mechanical Engineering, National Chiao Tung University, Hsinchu, Taiwan
[2]Department of Orthopaedics, Tzu Chi General Hospital, Taichung, Taiwan

The manuscript was received on 20 July 2008 and was accepted after revision for publication on 11 November 2008.

DOI: 10.1243/09544119JEIM476

Abstract: This study used finite element (FE) analysis with the load-controlled method (LCM) and the displacement-controlled method (DCM) to examine motion differences at the implant level and adjacent levels between fusion and non-fusion implants.

A validated three-dimensional intact (INT) L1–L5 FE model was used. At the L3–L4 level, the INT model was modified to surgery models, including the artificial disc replacement (ADR) of ProDisc II, and the anterior lumbar interbody fusion (ALIF) cage with pedicle screw fixation. The LCM imposed 10 N m moments of four physiological motions and a 150 N preload at the top of L1. The DCM process was in accordance with the hybrid testing protocol. The average percentage changes in the range of motion (ROM) for whole non-operated levels were used to predict adjacent level effects (ALE%).

At the implant level, the ALIF model showed similar stability with both control methods. The ADR model using the LCM had a higher ROM than the model using the DCM, especially in extension and torsion. At the adjacent levels, the ALIF model increased ALE% (at least 17 per cent) using the DCM compared with the LCM. The ADR model had an ALE% close to that of the INT model, using the LCM (average within 6 per cent), while the ALE% decreased when using the DCM.

The study suggests that both control methods can be adopted to predict the fusion model at the implant level, and similar stabilization characteristics can be found. The LCM will emphasize the effects of the non-fusion implants. The DCM was more clinically relevant in evaluating the fusion model at the adjacent levels. In conclusion, both the LCM and the DCM should be considered in numerical simulations to obtain more realistic data in spinal implant biomechanics.

Keywords: load-controlled method, displacement-controlled method, hybrid approach, finite element analysis, adjacent segment effect, artificial disc, fusion

1 INTRODUCTION

Spinal fusion is an effective surgical technique for treating low back pain [**1**]. However, clinical studies reported that the incidence of degeneration at adjacent levels after spinal fusion ranged from 6 per cent to 58 per cent of cases [**2–5**]. Patients may undergo another surgery for extended fusion to the adjacent levels, which is attributed to stress concentration at the adjacent levels and motion redistribution after rigid spinal fixation. Nowadays, the design concept of spinal implants has changed from traditional stable fusion to mobile non-fusion that attempts to restore normal physiological motion and to solve the adjacent segment problems [**6–9**].

In the past, several finite element (FE) and cadaver studies have used the traditional load-controlled method (LCM) to evaluate the characteristics of adjacent level effects (ALEs) on spinal constructs with fusion or non-fusion spinal implants [**6–8**, **10–14**]. This loading method applied the same pure

**Corresponding author: Department of Mechanical Engineering, National Chiao Tung University, 1001 Ta Hsueh Road, Hsinchu, Taiwan, 300, Republic of China. email: chhung@mail.nctu.edu.tw*

moment to all the spinal constructs, and then the motions in each level were calculated. However, conflicting results of ALEs were found with this type of analysis [**7**, **8**, **11**, **12**].

In recent years, Panjabi [**15**, **16**] introduced a new testing protocol that is similar to the displacement-controlled method (DCM), called the hybrid approach. This approach applies different moments so that the same overall ranges of motions (ROMs) are achieved for both intact and implant models. Goel and co-workers [**9**, **17**, **18**] indicated that, in real life, people bend their spines within a similar limited ROM regardless of whether their spine is healthy or has undergone spinal surgery. Therefore, they suggested that the hybrid approach should be more clinically relevant. Currently, a number of studies have evaluated spinal implant biomechanics using the hybrid approach [**9**, **16**, **17**, **19**]. However, only a few studies have focused on the differences between the LCM and DCM (hybrid approach). Goel *et al.* [**9**] analysed ALEs of artificial discs that used both the LCM and the hybrid approach, and revealed that ALEs were not obvious under the LCM, while the ALEs (in this case, decreased ROM) were significant under the hybrid approach. It is still not clear whether the LCM or the DCM is more suitable for revealing the reality of spinal implants. Therefore, this study used FE analysis with both the LCM and the DCM to explore biomechanical differences at the implant level and the adjacent levels between fusion and non-fusion spinal implants.

2 MATERIALS AND METHODS

Three FE models of the lumbar spine were constructed for this study. The first model was the intact lumbar spine. The other two models were the lumbar spine implanted with a SynCage-Open (Synthes Spine, Inc., Pennsyvlvania, USA) plus bilateral pedicle screws, and with a ProDisc II (Synthes, Inc., Paoli, Pennsylvania, USA; / Spine Solutions, New York, USA) artificial disc respectively. Two control methods, the LCM and the DCM, were included.

2.1 FE model of the intact lumbar spine

A three-dimensional non-linear intact lumbar spine (INT) L1–L5 FE model was constructed. The spinal geometry was obtained from 1 mm computed tomography scans of a middle-aged male, and the FE model was established using the software ANSYS 9.0 (ANSYS Inc., Canonsburg, Pennsylvania, USA) [**20**]. The INT model was an osseoligamentous lumbar spine as shown in Fig. 1(a), which included the vertebrae, intervertebral discs, endplates, posterior bony elements, and all seven ligaments.

An eight-node solid element (SOLID185) was used for modelling the cortical bone, cancellous bone, posterior bony element, cartilage endplate, and annulus ground substance. The cortical bone and cancellous bone were assumed to be homogeneous and transversely isotropic [**21**]. The posterior bony element and cartilage endplate were assumed to be homogeneous and isotropic [**22**]. The intervertebral disc consisted of annulus ground substance, nucleus pulposus, and collagen fibres embedded in the ground substance. The non-linear annulus ground substance was simulated by using a hyperelastic Mooney–Rivlin formulation [**23**, **24**]. This hyperelastic material model can simulate a non-linear stress–strain relationship, which is a material non-linear problem. The collagen fibres simply connected between nodes on adjacent endplates to create an irregular criss-cross configuration. These irregular angles of collagen fibres were oriented within the range of the study by Marchand and Ahmed [**25**]. In the radial direction, 12 double cross-linked fibre layers were defined to decrease the elastic strength proportionally from the outermost layer to the innermost. Therefore, the collagen fibres in different annulus layers were weighted. The elastic moduli at the outermost layers were as follows: layers 1 to 3, 1.0; layers 4 to 6, 0.9; layers 7 to 9; 0.75. The elastic modulus at the innermost layers 10 to 12 was 0.65. The cross-sectional areas at the outermost layers were as follows: layers 1 to 3, 1.0; layers 4 to 6, 0.78; layers 7 to 9, 0.62. The cross-sectional area at the innermost layers 10 to 12 was 0.47. These values were based on previous studies [**26**, **27**]. The nucleus pulposus was modelled as an incompressible fluid with a bulk modulus of 1666.7 MPa by eight-node fluid elements (FLUID80) [**22**, **28**]. All seven ligaments and collagen fibres were simulated by two-node bilinear link elements (LINK10) with uniaxial tension resistance only, which were arranged in an anatomically correct direction [**29**]. The cross-sectional area of each ligament was obtained from previous studies [**22**, **26**, **30**, **31**], and the material properties of the spine are listed in Table 1. The facet joint was treated as having sliding contact behaviour using three-dimensional eight-node surface-to-surface contact elements (CONTA174), which may slide between three-dimensional target elements (TARGE170). The coefficient of friction was set at 0.1 [**27**]. The initial gap between a pair of facet

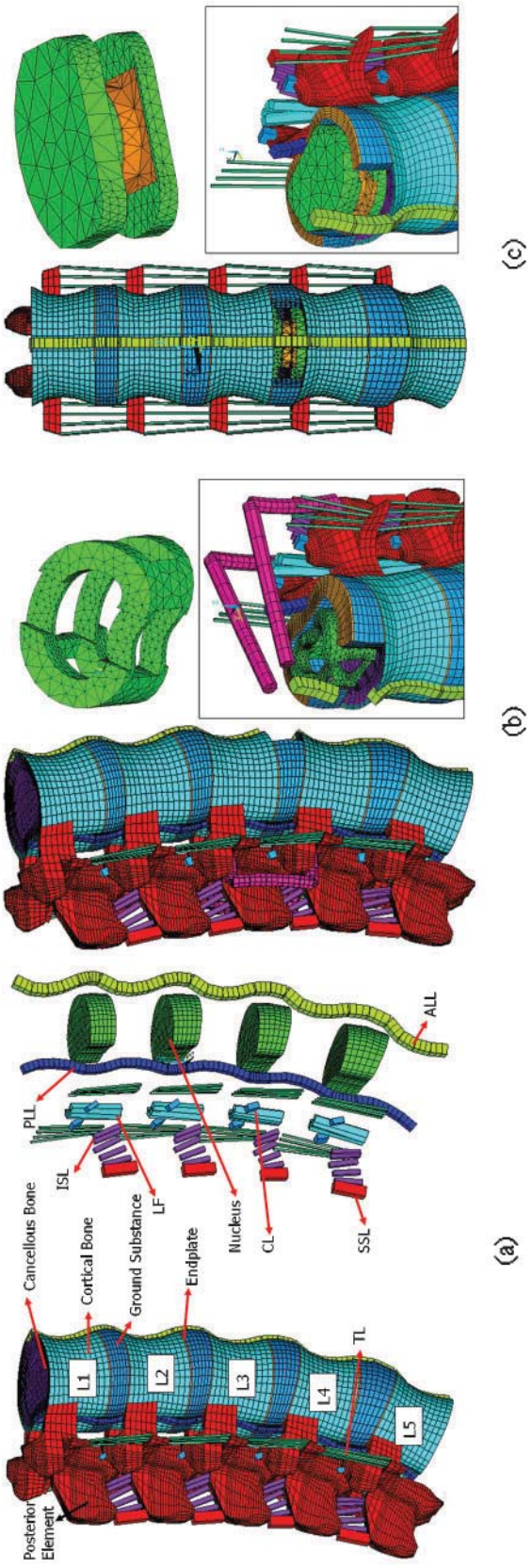

Fig. 1 FE model of the L1–L5 segments: (a) intact; (b) lumbar spine inserted SynCage-Open titanium cage supplemented with pedicle screws at L3–L4; (c) lumbar spine implanted ProDisc II artificial disc at L3–L4

Table 1 Material properties used in the FE model

Material	Element type	Young's modulus (MPa)	Poisson's ratio	Area (mm^2)	References
Bone		$E_x = 11\,300$	$v_{xy} = 0.484$	–	[**21**]
Cortical	Eight-node SOLID185	$E_y = 11\,300$	$v_{xz} = 0.203$		
		$E_z = 22\,000$	$v_{yz} = 0.203$		
		$G_x = 3800$			
		$G_y = 5400$			
		$G_z = 5400$			
Cancellous	Eight-node SOLID185	$E_x = 140$	$v_{xy} = 0.45$	–	[**21**]
		$E_y = 140$	$v_{xz} = 0.315$		
		$E_z = 200$	$v_{yz} = 0.315$		
		$G_x = 48.3$			
		$G_y = 48.3$			
		$G_z = 48.3$			
Posterior bone	Eight-node SOLID185	3500	0.25	–	[**22**]
Disc					
Nucleus pulposus	Eight-node FLUID80	1666.7	–	–	[**22**, **28**]
Ground substance	Eight-node SOLID185	$C_{10} = 0.42$	–	–	[**23**, **24**]
		$C_{01} = 0.105$			
Annulus fibres	Two-node LINK10				[**26**, **27**]
Outermost		550	–	0.76	
Second		495	–	0.5928	
Third		412.5	–	0.4712	
Innermost		357.5	–	0.3572	
Cartilaginous endplates	Eight-node SOLID185	24	0.4	-	[**22**]
Ligaments*	Two-node LINK10				[**22**, **26**, **30**, **31**]
ALL		7.8	–	24	
PLL		10	–	14.4	
TL		10	–	3.6	
LF		15	–	40	
ISL		10	–	26	
SSL		8	–	23	
CL		7.5	–	30	
Spinal instrumentation (titanium alloy)	Two-node BEAM188	110 000	0.28	$D = 6$ mm	
SynCage-Open (titanium alloy)	Eight-node SOLID185	110 000	0.28	–	
ProDisc II metallic endplate (Co-Cr-Mo alloy)	Eight-node SOLID185	210 000	0.3	–	
Polyethylene inlay ultra-high molecular weight polyethylene	Eight-node SOLID185	1016	0.46	–	[**32**]

*ALL, anterior longitudinal ligament; PLL, posterior longitudinal ligament; TL, transverse ligament; LF, ligamentum flavum; ISL, interspinous ligament; SSL, supraspinous ligament; CL, capsular ligament.

surfaces was kept within 0.5 mm [**22**]. The stiffness of the spinal structure changes depending on the contact status, and so the standard contact option in ANSYS was adopted to account for the changing-states non-linear problem in this study. In addition, the element's shape will change after applying bending moments, thus changing the individual element stiffness. Therefore, the large displacement analysis option in ANSYS was chosen to solve this geometric non-linear problem. The INT model consisted of 112 174 elements and 94 162 nodes (Fig. 1(a)).

2.2 FE model of the anterior lumbar interbody fusion

To simulate the anterior lumbar interbody fusion (ALIF), the L3–L4 level of the INT model underwent partial discectomy and total nuclectomy by the anterior approach, which included removal of the anterior longitudinal ligament, anterior and some inner layer portions of the annulus, and the entire nucleus pulposus. All the other ligaments were preserved. Next, an 8° lordotic titanium alloy cage (SynCage-Open; 30 mm × 24 mm × 21 mm) supplemented with bilateral pedicle screw fixation was inserted. The material properties of the cage and posterior implant system are listed in Table 1.

In this model, four pedicle screws ($r = 3$ mm) and two rods ($r = 3$ mm) were modelled with three-dimensional beam elements (BEAM188); then a full constraint behaviour was designed between the screw–bone interface to simulate the pedicle screw bounded on the vertebrae. A SynCage was placed between the vertebral bodies, and the bone–cage interfaces were assigned fully bonded conditions to mimic successful fusion. The ALIF model consisted of 139 692 elements and 99 924 nodes (Fig. 1(b)).

2.3 FE model of the anterior lumbar artificial disc replacement

To simulate the artificial disc replacement (ADR), a ProDisc II was implanted into the INT model at L3–L4 following the standard ADR procedure. The anterior and inner layer portions of annulus at L3–L4 were removed. In addition, the nucleus of L3–L4 was totally removed and all spinal ligaments were preserved. Figure 1(c) shows the remaining disc annulus and spinal ligaments after implanting ProDisc II. The material properties of the ProDisc II are listed in Table 1.

The keel of the metallic plate surfaces was modelled as a flat surface for simplification. A fully bonded condition was applied between the metallic plate and adjacent vertebrae. Deformable surface-to-surface contact behaviour was used between the polyethylene inlay and the superior metallic plate, and the coefficient of friction for the polyethylene–(Co–Cr–Mo) alloy contact surface was chosen to be 0.07 [**32**]. The ADR model consisted of 113 315 elements and 91 126 nodes (Fig. 1 (c)).

2.4 Convergence test and model validation

In order to obtain reliable data, model validation and a convergence test were conducted. For the convergence test, three mesh densities (coarse model, 4750 elements and 4960 nodes; normal model, 27 244 elements and 30 630 nodes; finest model, 112 174 elements and 94 162 nodes) were selected to test for ROM changes in the INT model, and the finest mesh density was chosen since the change was within 1.03 per cent (less than 0.2°).

For the model validation, the loading condition was based on an *in vitro* study in which the multi-level lumbar spine was subjected to the maximum possible load without causing spinal injury [**33**]. Therefore, the LCM was used to validate all four physiological motions, i.e. flexion, extension, torsion, and lateral bending. In each case a moment of 10 N m and a preload of 150 N were placed on the superior surface at the L1 level. In addition, the pure moments of 3.5 N m and 7.5 N m were also used in validating the INT model. These models constrained all degrees of freedom at the inferior surfaces of the L5 vertebra.

2.5 Boundary and loading conditions

The LCM and DCM were used to explore the differences at the implant and the adjacent levels. The LCM was the same control method that had been used in the model validation (10 N m with 150 N preload). For the DCM, a 150 N preload was applied on the superior surface of the L1 vertebra, and then a higher pure moment of 30 N m was applied incrementally by 0.3 N m in 100 loading steps. The result of every substep was saved. Therefore, the resultant ROMs (L1 to L5) of the ALIF and ADR models under different moments would match the ROMs of the INT model by using the LCM. The detailed total lumbar ROMs of the INT model under the LCM are 16.84° in flexion, 14.73° in extension, 9.48° in torsion, and 17.14° in lateral bending (Table 2). These ROMs are a baseline to match the total lumbar motion among the INT and surgical models under DCM (Table 3). The resulting deviation of ROMs among the three FE models were controlled to

Table 2 Intervertebral range of motion and applied moment among the INT, ALIF, and ADR models under the LCM

	ROM (deg)				Total lumbar ROM (deg) (L1–L5)	Moment (N m)
	L1–L2	L2–L3	L3–L4	L4–L5		
Flexion						
INT	3.76	3.93	4.00	5.15	16.84	10
ALIF	4.01	4.21	0.09	6.04	14.35	10
ADR	3.76	3.86	4.37	5.23	17.22	10
Extension						
INT	3.30	3.37	3.70	4.36	14.73	10
ALIF	3.14	3.03	0.42	4.06	10.65	10
ADR	3.69	3.54	6.69	4.37	18.29	10
Torsion						
INT	2.03	2.16	2.50	2.79	9.48	10
ALIF	2.05	2.05	1.07	2.72	7.89	10
ADR	2.09	2.09	4.19	2.73	11.10	10
Lateral bending						
INT	3.97	4.05	4.25	4.87	17.14	10
ALIF	4.13	4.24	1.15	5.28	14.80	10
ADR	3.80	3.80	6.14	4.66	18.40	10

Table 3 Intervertebral range of motion and applied moment among the INT, ALIF, and ADR models under the DCM

	ROM (deg)				Total lumbar ROM (deg) (L1–L5)	Moment (N m)
	L1–L2	L2–L3	L3–L4	L4–L5		
Flexion						
INT	3.76	3.93	4.00	5.15	16.84	10
ALIF	4.69	4.92	0.65	6.55	16.81	12.9
ADR	3.65	3.76	4.25	5.08	16.74	9.6
Extension						
INT	3.30	3.37	3.70	4.36	14.73	10
ALIF	4.38	4.24	0.65	5.55	14.82	16.2
ADR	2.95	2.91	5.36	3.64	14.86	6.9
Torsion						
INT	2.03	2.16	2.50	2.79	9.48	10
ALIF	2.46	2.46	1.31	3.20	9.43	13.2
ADR	1.72	1.85	3.56	2.37	9.50	7.8
Lateral bending						
INT	3.97	4.05	4.25	4.87	17.14	10
ALIF	4.89	4.92	1.31	6.02	17.14	12.3
ADR	3.26	3.57	5.82	4.41	17.06	9

within 0.1° in flexion, 0.13° in extension, 0.05° in torsion, and 0.08° in lateral bending. The above procedure used in this study was in accordance with the hybrid testing protocol that was presented in detail in several previous studies [**9**, **15**, **16**]. With both control methods, all the models were constrained at the bottom of the fifth vertebra.

3 RESULTS

The results are revealed in four parts. First, the model validation is presented. Second, the implant level effects are shown. Third, the ALEs on the fusion and non-fusion spinal construct are compared with those of the intact lumbar spine under both loading conditions. Fourthly, the stress variation in the adjacent disc annulus is revealed under both control methods. In this study, the data were normalized to the INT model as percentage values under each loading mode.

3.1 Model validation results

The ROMs in five levels of the INT model under different loading moments were validated with previous *in-vitro* cadaveric tests and analytical studies [**33–36**] (Fig. 2). Under a 10 N m moment with a 150 N preload, the current INT model showed some stiffer behaviour in flexion and exhibited a 6–11° lower ROM value than those obtained by Yamamoto *et al.* [**33**] and Panjabi *et al.* [**35**] *in-vitro* studies, as shown in Fig. 2(a). In torsion, the difference between the INT model and the *in-vitro* tests was less than 2°. Under 3.75 N m and 7.5 N m pure moments, all the five lumbar ROMs were within the range of extreme values in flexion–extension, both side torsions, and both side lateral bendings, compared with the results of an *in-vitro* test without a follower load made by Rohlmann *et al.* [**36**] (Fig. 2(b)).

3.2 Implant level effects

Under the LCM, the ALIF model showed relative stability, compared with the INT model; the ROM was reduced significantly in flexion (−97.7 per cent), extension (−88.6 per cent), and lateral bending (−72.9 per cent), but less in torsion (−57.0 per cent), compared with the INT model. In contrast, the ADR model had a large ROM increase in extension (+81.1 per cent) (Fig. 4(a)), torsion (+67.9 per cent) (Fig. 5(a)), and lateral bending (+44.5 per cent) (Fig. 6(a), but less in flexion (+9.2 per cent) (Fig. 3(a)). The ROM values of the LCM are listed in Table 2.

Under the DCM, the ROM of the ALIF model was reduced significantly in flexion (−83.7 per cent), extension (−82.4 per cent), and lateral bending (−69.2 per cent), but less in torsion (−47.6 per cent), compared with the INT model. In contrast, the ADR model had a large ROM increase in extension (+45.1 per cent) (Fig. 4(b)), torsion (+42.7 per cent) (Fig. 5(b)), and lateral bending (+37.1 per cent) (Fig. 6(b)), but less in flexion (+6.4 per cent) (Fig. 3(b)). The ROM values of the DCM are listed in Table 3.

Both control methods can provide similar stability in the ALIF model. However, in the ADR model, the LCM showed prominently higher ROM than the DCM, especially in extension and torsion.

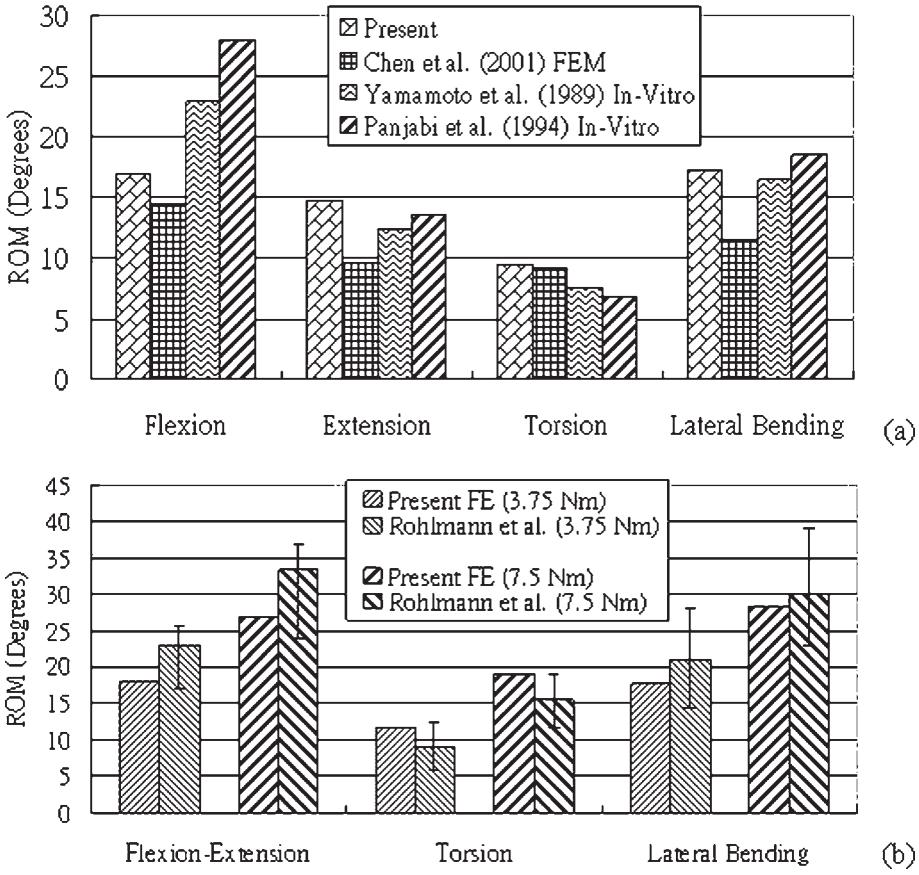

Fig. 2 Comparison of ROM calculated for the five levels of intact lumbar spine with previous *in-vitro* experiments and analytical studies: (a) loading of 10 N m moments with 150 N preload in the present INT model; (b) loading of 3.75 N m and 7.5 N m pure moments in the present INT model. (The data in (b) include both side motions. Median and extreme values for the *in vitro* data are shown)

3.3 Adjacent level effects

The ALE% was defined as the averaged percentage changes of the ROM from whole non-operated levels. Under the LCM, the ALE% of the ALIF model in flexion (+10.3 per cent) and extension (−7.3 per cent) were small, and in torsion and lateral bending were even smaller (average within 6 per cent). The ALE% values of the ADR model were close to those of the INT model in flexion (Fig. 3(a)), extension (Fig. 4(a)), torsion (Fig. 5(a)), and lateral bending (Fig. 6(a)) (average within 6 per cent).

Under the DCM, the ALE% of the ALIF model increased in flexion (+25.6 per cent), extension (+28.6 per cent), torsion (+16.7 per cent), and lateral bending (+22.8 per cent), compared with the INT model. In contrast, the ALE% of the ADR model decreased significantly in extension (−13.6 per cent) (Fig. 4(b)), torsion (−14.9 per cent) (Fig. 5(b)), and lateral bending (−13.0 per cent) (Fig. 6(b)), but less in flexion (−2.9 per cent) (Fig. 3(b)), compared with those with the INT model.

The DCM increased the ALE% more than when using the LCM in the ALIF model; on the other hand, the DCM decreased the ALE% more than when using the LCM in the ADR model, especially in extension, torsion, and lateral bending.

3.4 Stress and intradiscal pressure variation in the adjacent disc

Under the LCM, the intradiscal pressure of the ALIF and ADR models at the adjacent L2–L3 level changed by −18.3 per cent and by +3.5 per cent in flexion. In contrast, under the DCM, the intradiscal pressure of the ALIF and ADR models at the adjacent L2–L3 level changed by +8.5 per cent and by +0.7 per cent in flexion. Therefore, the ALIF model slightly raised intradiscal pressure at the adjacent L2–L3 level under the DCM. The intradiscal pressure of the ADR model showed only minor changes between both control methods.

Figure 7 indicates the stress distribution of the L2–L3 annulus in the LCM or the DCM among the

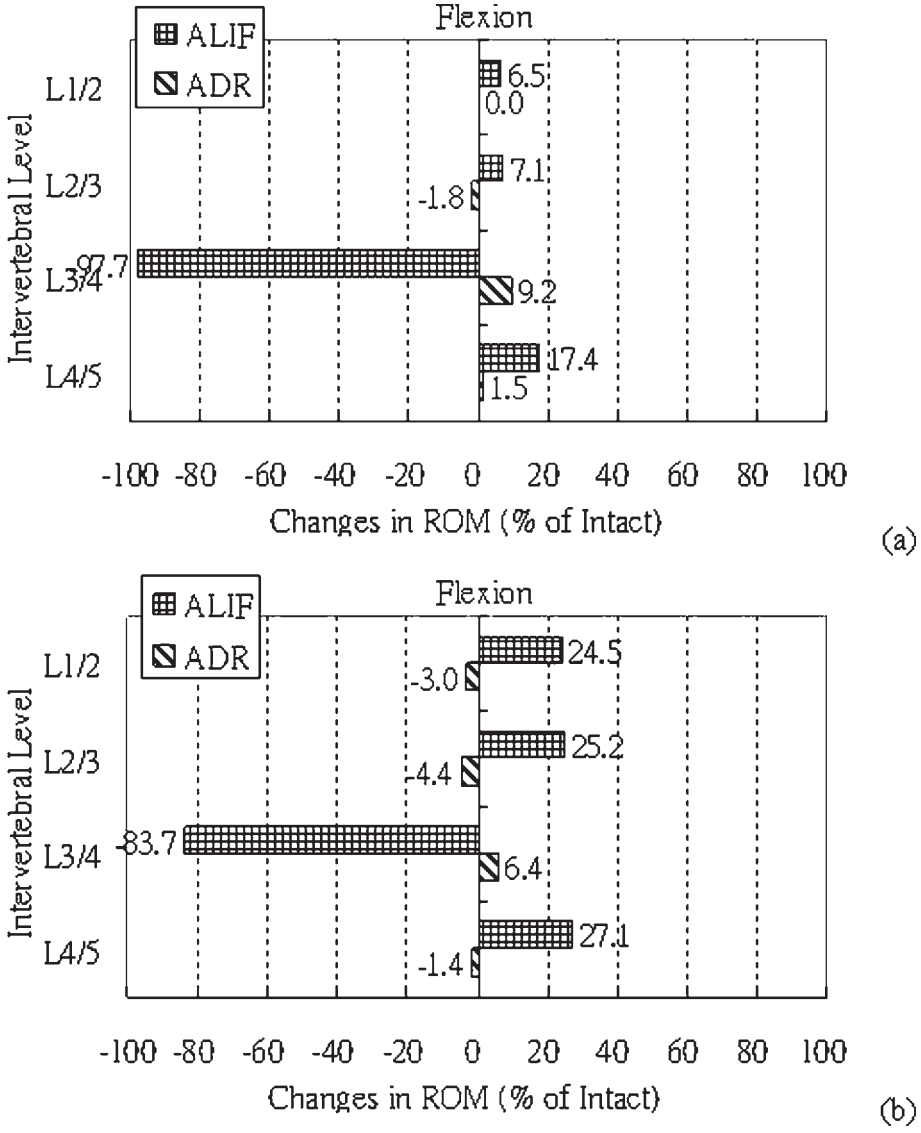

Fig. 3 Changes in the ROM under flexion: (a) LCM results; (b) DCM results

three FE models (flexion). For the DCM, a higher stress concentration at the adjacent level after a fusion procedure is more clearly shown, compared with the LCM. The same stress trends were also found in three other physiological motions. These results indicated that use of the DCM in evaluating the adjacent level should be more clinically relevant.

4 DISCUSSION

Accelerative degeneration of adjacent levels is an important clinical issue after spinal fusion. Different testing methods have been used to evaluate ALEs after implanting various spinal implants [**16**]. However, it is still not clear which testing method is more suitable for revealing the reality of spinal implants. This study aimed to evaluate the differences of the LCM and DCM FE analyses applied to fusion and non-fusion implants.

For the INT model, the present FE simulation is in good agreement with *in-vitro* tests in terms of extension, torsion, and lateral bending [**33**, **35**], whereas the ROM is 6–11° lower than that from the *in-vitro* test under flexion. Eberlein *et al.* [**37**] also indicated that the numerical results exhibited a response that was stiffer than the experimental results in terms of flexion using the same moment. Their study also indicated that these deviations can be reduced by assuming tissue degeneration in the annulus fibrosus and a complete loss of intradiscal pressure in the intervertebral discs. Therefore, tissue degeneration plays an important role in the motion

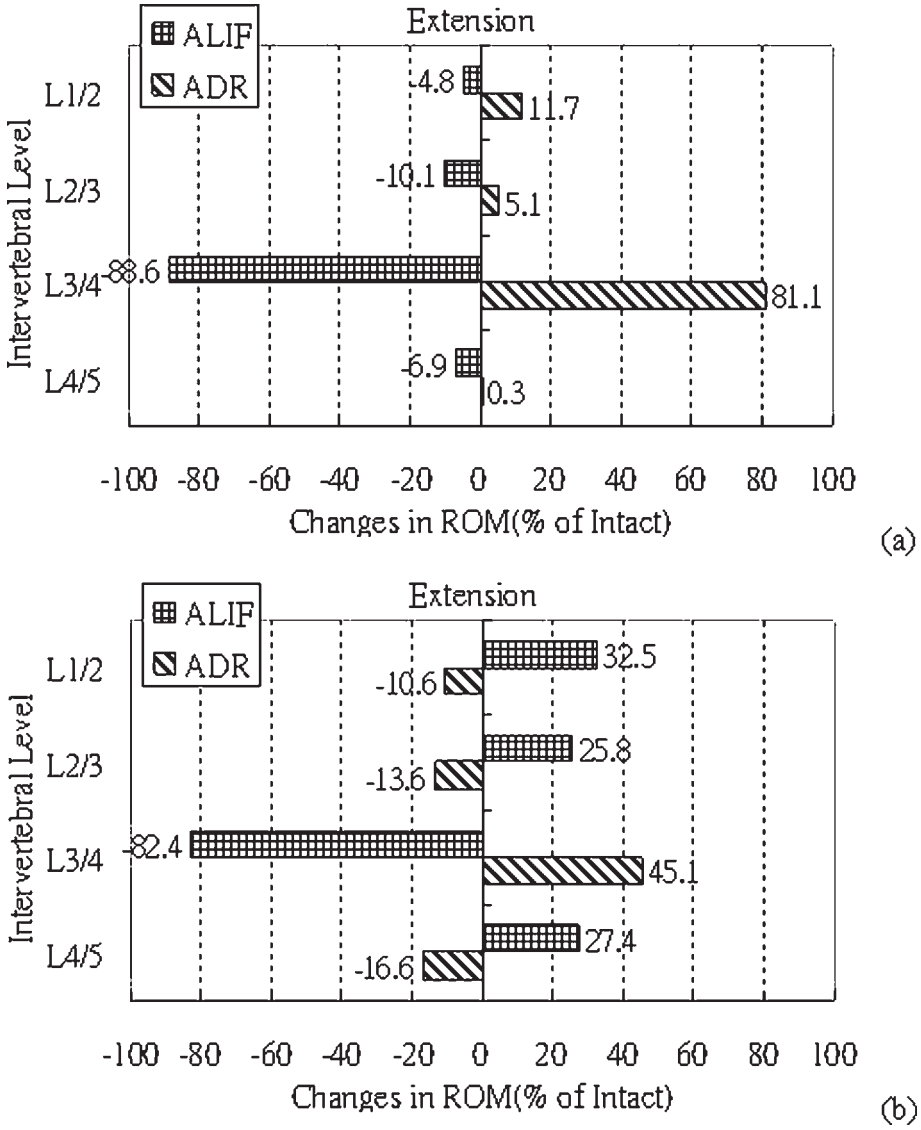

Fig. 4 Changes in the ROM under extension: (a) LCM results; (b) DCM results

behaviour of the lumbar spine. In the *in-vitro* test made by Rohlmann *et al.* [**36**], the older cadaver specimens revealed a larger variance in ROM than younger specimens did. This discrepancy in flexion may be the result of various stages of disc degeneration, such as microfissures in the disc, annulus bulging, damage to the endplate, or dehydration of the disc. Furthermore, specimens could possibly have suffered soft-tissue decay after a longer experimental time, and this may have caused extreme stiffness changes in the specimens. Therefore, the cadaveric specimen of the *in-vitro* tests exhibited lower stiffness than the FE spine model analysis in flexion.

For the implant level, the ALIF model showed similar stability with both control methods. Oxland and Lund [**38**] indicated that anterior fusion plus posterior pedicle screw fixation can improve stabilization in all motions. Gerber *et al.* [**39**] indicated that anterior cage plus posterior pedicle screw fixation did not provide significant stability in torsion with the LCM. This behaviour of the LCM is similar to the *in-vitro* test of Panjabi *et al.* [**40**] using the hybrid method, in which the ROM decreased by 77.4 per cent in flexion–extension, by 36.4 per cent in torsion, and by 65.7 per cent in lateral bending. The results of this study are in agreement with most of the *in-vitro* test results [**38**–**41**], in that the fusion level can provide good stability in flexion, extension, and lateral bending but is not so in torsion, regardless of whether the LCM or DCM is used.

The implant level of the ADR model shows significantly increased ROM in extension, torsion,

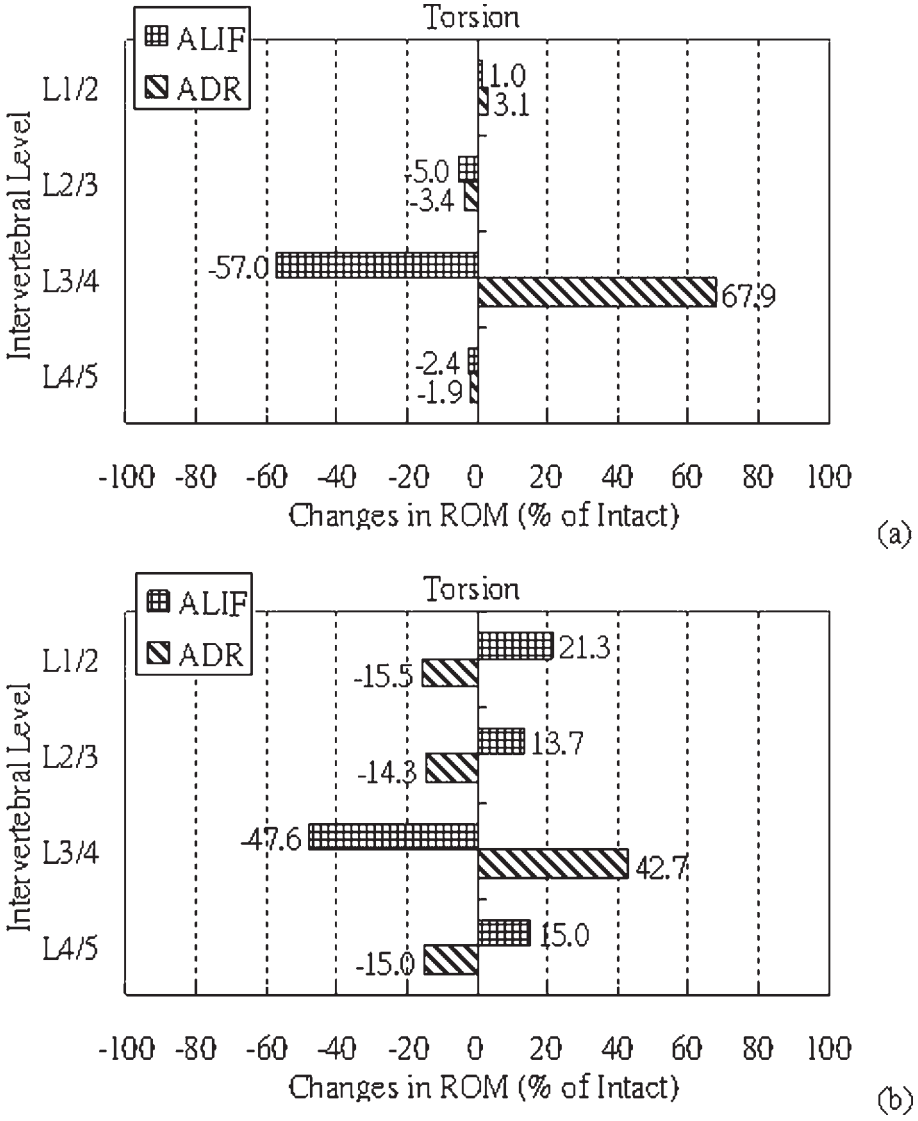

Fig. 5 Changes in the ROM under torsion: (a) LCM results; (b) DCM results

and lateral bending under both control methods. In addition, the LCM showed higher ROM than the DCM, especially in extension and torsion. These characteristics of the ADR are in agreement with a previous report by Goel *et al.* [**9**].

Therefore, this study suggests that both control methods can be adopted to evaluate the implant level of the fusion model, and similar stabilizing characteristics can be expected to be found. On the other hand, the effects on the implant level of the ADR increased ROM with the LCM, especially in extension (81.1 per cent versus 45.1 per cent) and torsion (67.9 per cent versus 42.7 per cent). Thus, LCM analysis might indicate a higher risk for patients with ADR implants. The present authors believe that the LCM emphasizes the effects on the implant level of the non-fusion implant.

For the adjacent levels, the ALIF model shows a significantly increased ALE%, using the DCM. As mentioned previously, conflicting ALE% results were found with the LCM. The ALE% of the DCM determined in the current study are in the range of the values reported in the literature [**19**, **40**, **41**], which showed a significantly increased ALE%. However, a few inconsistencies in the ALE% were still noticed. In lateral bending, significantly increased ALE% with fusion was reported (average, +20.7 per cent) [**19**]; in contrast, a small ALE% with fusion was also found (average, +4.1 per cent) [**40**]. This discrepancy was also revealed in torsion [**19**, **40**, **41**]. Despite these differences in ALEs, this study has shown that the DCM could emphasize the ALEs more than the LCM on the fusion model. Figure 7 indicates that the stress distribution on the adjacent

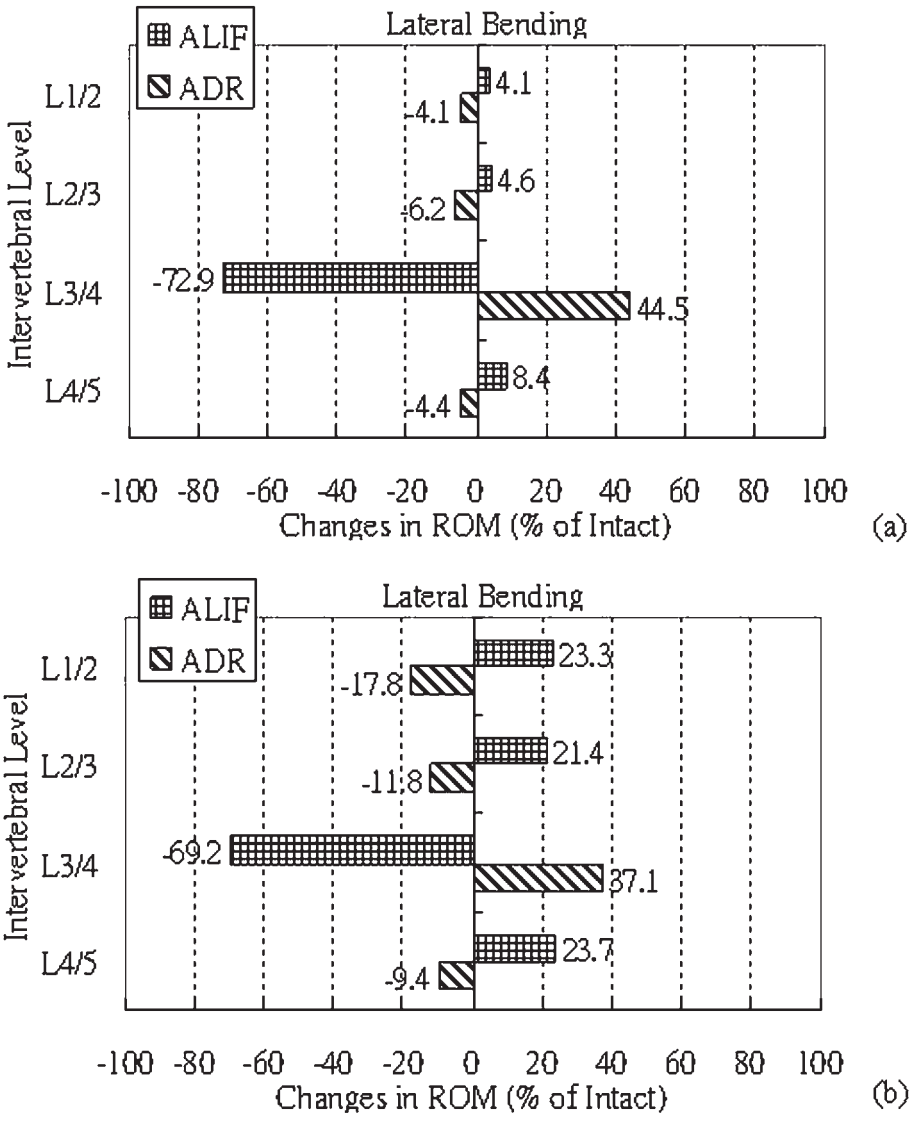

Fig. 6 Changes in the ROM under lateral bending: (a) LCM results; (b) DCM results

disc annulus increased markedly in the DCM after the fusion procedure. Clinical reports showed that high incidences of accelerative disc degeneration and facet joint arthritis at the adjacent levels were present [**2**, **4**, **42**, **43**]. Based on these observations, the DCM is more effective in predicting the ALEs after spinal fusion.

The ALE% of the ADR model in adjacent levels was close to the INT model with the LCM, while it was significantly decreased with the DCM. This trend of an ALE% decrease was also found in other studies using the hybrid method [**9**, **40**, **41**]. The intradiscal pressure of the ADR model changed only to a minor extent at the adjacent L2–L3 level (less than 4 per cent). This trend is in agreement with the findings of previous studies [**9**, **44**].

Overall, this study suggests that the DCM should be more clinically relevant in evaluating the ALEs of the fusion model. On the other hand, the DCM may decrease the ALEs of the ADR. Verification of the influence of these abnormal motions requires more evidence through clinical research. Therefore, the conclusion was reached that both control methods should be used in evaluating ALEs of non-fusion implants.

Goel *et al.* [**9**] proposed that the patient's main aim following surgery is to go back to normal daily life. Thus, the surgically treated spine should be able to go through the same ROM as in a normal person. However, in real life, people sustain the same external moments during lifting activities, whether or not they have had surgery, thus the LCM is useful

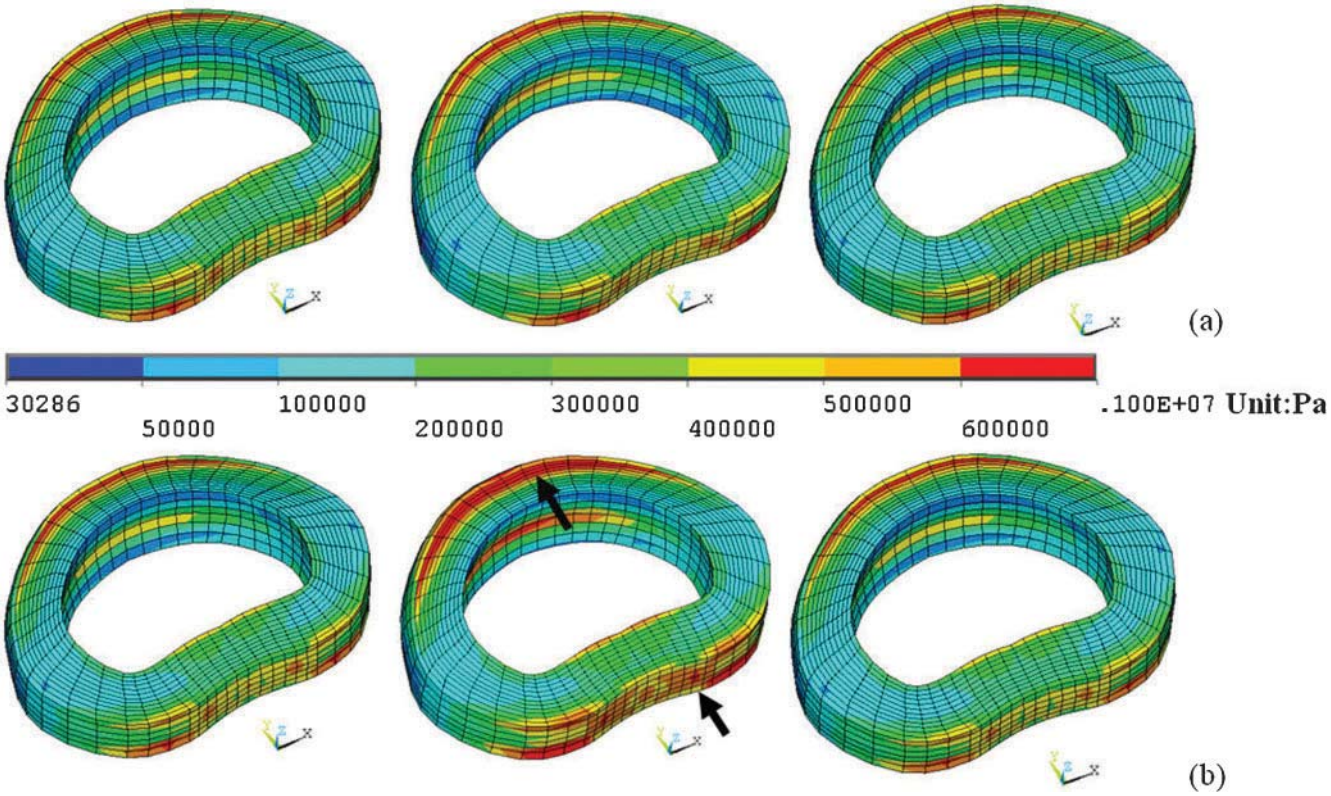

Fig. 7 Von Mises stress distribution of the adjacent L2–L3 disc annulus under flexion for the INT model (left), the ALIF model (middle), and the ADR model (right): (a) LCM; (b) DCM. The solid arrows indicate stress concentration regions

for evaluating this condition. The present authors believe that these two analytical methods could be used to predict specific conditions in the patient's daily life. The DCM is suitable for evaluating the patient's daily life motion during restoration after surgery, while the LCM is suitable for evaluating the patient's normal life work-loading condition after surgery [**45**].

One limitation of this study is that the material properties of this simulation, such as the non-linear behaviour of the spinal ligaments, the viscoelasticity of the disc, and the grade of degenerative disc, were slightly simplified and idealized from those of a cadaver specimen. A degenerative disc is common in most patients before surgery. The various grades of degeneration in the disc, such as delamination, dehydration, or reduced disc height, do not allow for exact replication of the unique material properties of a degenerated disc. Therefore, normal material properties were used in this simulation. Also, the constrained behaviour used in the bone–screw interface, the keel in the metallic plates of the ProDisc, and the bone ingrowth into the cage were simplified. Pretension should occur after inserting the ADR, which might distract the remaining annulus, reducing the ROM and facet loading at the surgical level. This mechanism was not modelled here, which is a limitation in this study. The loading conditions of these FE simulations were similar to those of the traditional *in-vitro* test; so the muscle contraction, complicated external load, and movement of the pelvis were not considered in this study. In daily life activities, muscles induce considerably high compression forces on the lumbar spine [**46**], and muscles play a very important role in stabilizing the lumbar spine [**47**]. The absence of muscle forces would lead to more instability, especially at the surgical level of surgery models. In addition, the annulus stress, intradiscal pressure, and implant loading would be much lower than those measured *in vivo*. Patwardhan *et al.* [**48**] proposed a follower load to mimic the more realistic physiological compressive loads seen *in vivo*. This consists of a compressive load applied along a follower load path that approximates the tangent to the curve of the lumbar spine, thus subjecting the whole lumbar

spine to nearly pure compression. In this study, this condition was not a matter of concern. However, an FE analytical study with a follower load on fusion and non-fusion spinal implants will be presented in the near future.

5 CONCLUSION

In this research, differences between the LCM and DCM FE analyses for the evaluation of fusion and non-fusion implants were observed. For the implant level, this study suggests that both control methods can be adopted to predict the fusion model, and similar stabilization characteristics can be found. The LCM will emphasize the effects of the non-fusion implant. For the adjacent levels, the DCM was more clinically relevant in evaluating the fusion model. These two analytical methods can be used to predict specific conditions in a patient's daily life. The DCM is suitable for evaluation of the patient's daily life motion during restoration after surgery. The LCM is suitable for evaluation of the patient's normal life work-loading condition after surgery.

REFERENCES

1 **Fritzell, P., Hagg, O., Wessberg, P., Nordwall, A.,** and **The Swedish Lumbar Spine Study Group.** 2001 volvo award winner in clinical studies: lumbar fusion versus nonsurgical treatment for chronic low back pain — a multicenter randomized controlled trial from the Swedish lumbar spine study group. *Spine*, 2001, **26**(23), 2521–2534.

2 **Lee, C. K.** Accelerated degeneration of the segment adjacent to a lumbar fusion. *Spine*, 1988, **13**(3), 375–377.

3 **Lehmann, T. R., Spratt, K. F., Tozzi, J. E., Weinstein, J. N., Reinarz, S. J., El-Khoury, G. Y.,** and **Colby, H.** Long-term follow-up of lower lumbar fusion patients. *Spine*, 1987, **12**(2), 97–104.

4 **Rahm, M. D.** and **Hall, B. B.** Adjacent segment degeneration after lumbar fusion with instrumentation: a retrospective study. *J. Spinal Disorders*, 1996, **9**(5), 392–400.

5 **Kuslich, S. D., Danielson, G., Dowdle, J. D., Sherman, J., Fredrickson, B., Yuan, H.,** and **Griffith, S. L.** Four-year follow-up results of lumbar spine arthrodesis using the Bagby and Kuslich lumbar fusion cage. *Spine*, 2000, **25**(20), 2656–2662.

6 **Lafage, V., Gangnet, N., Senegas, J., Lavaste, F.,** and **Skalli, W.** New interspinous implant evaluation using an *in vitro* biomechanical study combined with finite-element analysis. *Spine*, 2007, **32**(16), 1706–1713.

7 **Schmoelz, W., Huber, J. F., Nydegger, T., Claes, L.,** and **Wilke, H. J.** Influence of a dynamic stabilization system on load bearing of a bridged disc: an *in vitro* study of intradiscal pressure. *Eur. Spine J.*, 2006, **15**(8), 1276–1285.

8 **Cunningham, B. W., Gordon, J. D., Dmitriev, A. E., Hu, N.,** and **McAfee, P. C.** Biomechanical evaluation of total disc replacement arthroplasty: an *in vitro* human cadaveric model. *Spine*, 2003, **28**(20S), S110–S117.

9 **Goel, V. K., Grauer, J. N., Patel, T., Biyani, A., Sairyo, K., Vishnubhotla, S., Matyas, A., Cowgill, I., Shaw, M., Long, R., Dick, D., Panjabi, M. M.,** and **Serhan, H.** Effects of Charite artificial disc on the implanted and adjacent spinal segments mechanics using a hybrid testing protocol. *Spine*, 2005, **30**(24), 2755–2769.

10 **Vadapalli, S., Sairyo, K., Goel, V. K., Robon, M., Biyani, A., Khandha, A.,** and **Ebraheim, N. A.** Biomechanical rationale for using polyetheretherketone (PEEK) spacers for lumbar interbody fusion — a finite element study. *Spine*, 2006, **31**(26), E992–E998.

11 **Sudo, H., Oda, I., Abumi, K., Ito, M., Kotani, Y.,** and **Minami, A.** Biomechanical study on the effect of five different lumbar reconstruction techniques on adjacent-level intradiscal pressure and lamina strain. *J. Neurosurg. Spine*, 2006, **5**(2), 150–155.

12 **Denoziere, G.** and **Ku, D. N.** Biomechanical comparison between fusion of two vertebrae and implantation of an artificial intervertebral disc. *J. Biomechanics*, 2006, **39**(4), 766–775.

13 **Wang, S. T., Goel, V. K., Fu, C. Y., Kubo, S., Choi, W., Liu, C. L.,** and **Chen, T. H.** Posterior instrumentation reduces differences in spine stability as a result of different cage orientations: an *in vitro* study. *Spine*, 2004, **30**(1), 62–67.

14 **Hitchon, P. W., Goel, V., Rogge, T., Dooris, A., Drake, J.,** and **Torner, J.** Spinal stability with anterior or posterior ray threaded fusion cages. *J. Neurosurg.*, 2000, **93**(Suppl. 1), 102–108.

15 **Panjabi, M. M.** Biomechanical testing to identify adjacent-level effects. In Proceedings of the Fourth World Congress of Biomechanics, Calgary, Alberta Canada, 4–9 August 2002.

16 **Panjabi, M. M.** Hybrid multidirectional test method to evaluate spinal adjacent-level effects. *Clin. Biomechanics*, 2007, **22**(3), 257–265.

17 **Grauer, J. N., Biyani, A., Faizan, A., Kiapour, A., Sairyo, K., Ivanov, A., Ebraheim, N. A., Patel, T. C.,** and **Goel, V. K.** Biomechanics of two-level Charite artificial disc placement in comparison to fusion plus single-level disc placement combination. *Spine J.*, 2006, **6**(6), 659–666.

18 **Goel, V. K., Panjabi, M. M., Patwardhan, A. G., Dooris, A. P.,** and **Serhan, H.** Test protocols for evaluation of spinal implants. *J. Bone Jt Surg. Am.*, 2006, **88**(Suppl. 2), 103–109.

19 **Panjabi, M. M., Henderson, G., James, Y.,** and **Timm, J. P.** StabilimaxNZ versus simulated fusion:

evaluation of adjacent-level effects. *Eur. Spine J.*, 2007, **16**(12), 2159–2165.

20 *ANSYS 9.0 user's manual*, 2004 (ANSYS Inc., Canonsburg, Pennsylvania).

21 **Lu, Y. M., Hutton, W. C.,** and **Gharpuray, V. M.** Do bending, twisting, and diurnal fluid change in the disc affect the propensity to prolapse? A visco-elastic finite element model. *Spine*, 1996, **21**(22), 2570–2579.

22 **Goel, V. K., Monroe, B. T., Gilbertson, L. G.,** and **Brinckmann, P.** Interlaminar shear stresses and laminae separation in a disc. Finite element analysis of the L3–L4 motion segment subjected to axial compressive loads. *Spine*, 1995, **20**(6), 689–698.

23 **Rohlmann, A., Zander, T.,** and **Bergmann, G.** Effects of total disc replacement with ProDisc on intersegmental rotation of the lumbar spine. *Spine*, 2005, **30**(7), 738–743.

24 **Schmidt, H., Heuer, F., Simon, U., Kettler, A., Rohlmann, A., Claes, L.,** and **Wilke, H. H.** Application of a new calibration method for a three-dimensional finite element model of a human lumbar annulus fibrosus. *Clin. Biomechanics*, 2006, **21**(4), 337–344.

25 **Marchand, F.** and **Ahmed, A. M.** Investigation of the laminate structure of lumbar disc annulus fibrosus. *Spine*, 1990, **15**(5), 402–410.

26 **Shirazi-Adl, A., Ahmed, A. M.,** and **Shrivastava, S. C.** Mechanical response of a lumbar motion segment in axial torque alone and combined with compression. *Spine*, 1986, **11**(9), 914–927.

27 **Polikeit, A., Ferguson, S. J., Nolte, L. P.,** and **Orr, T. E.** Factors influencing stresses in the lumbar spine after the insertion of intervertebral cages: finite element analysis. *Eur. Spine J.*, 2003, **12**(2), 413–420.

28 **Rohlmann, A., Zander, T.,** and **Bergmann, G.** Effects of fusion-bone stiffness on the mechanical behavior of the lumbar spine after vertebral body replacement. *Clin. Biomechanics*, 2006, **21**(3), 221–227.

29 **Agur, A. M. R.** and **Lee, M. J.** *Grant's atlas of anatomy*, 10th edition, 1999 (Lippincott Williams & Wilkins, Philadelphia, Pennsylvania).

30 **White III, A. A.** and **Panjabi, M. M.** *Clinical biomechanics of the spine*, 2nd edition, 1990 (J. B. Lippincott Company, Philadelphia, Pennsylvania).

31 **Lee, K. K., Teo, E. C., Fuss, F. K., Vanneuville, V., Qiu, T. X., Ng, H. W., Yang, K.,** and **Sabitzer, R. J.** Finite-element analysis for lumbar interbody fusion under axial loading. *IEEE. Trans. Biomed. Engng*, 2004, **51**(3), 393–400.

32 **Godest, A. C., Beaugonin, M., Haug, E., Taylor, M.,** and **Gergson, P. J.** Simulation of a knee joint replacement during a gait cycle using explicit finite element analysis. *J. Biomechanics*, 2002, **35**(2), 267–275.

33 **Yamamoto, I., Panjabi, M. M., Crisco, T.,** and **Oxland, T.** Three-dimensional movements of the whole lumbar spine and lumbosacral joint. *Spine*, 1989, **14**(11), 1256–1260.

34 **Chen, C. S., Cheng, C. K., Liu, C. L.,** and **Lo, W. H.** Stress analysis of the disc adjacent fusion in lumbar spine. *Med. Engng Physics*, 2001, **23**(7), 483–491.

35 **Panjabi, M. M., Oxland, T. R., Yamamoto, I.,** and **Crisco, J. J.** Mechanical behavior of the human lumbar and lumbosacral spine as shown by three-dimensional load–displacement curves. *J. Bone Jt Surg. Am.*, 1994, **76**(3), 413–424.

36 **Rohlmann, A., Neller, S., Claes, L., Bergmann, G.,** and **Wilke, H. J.** Influence of a follower load on intradiscal pressure and intersegmental rotation of the lumbar spine. *Spine*, 2001, **26**(24), E557–E561.

37 **Eberlein, R., Holzapfel, A.,** and **Frohlich, M.** Multi-segment FEA of the human lumbar spine including the heterogeneity of the annulus fibrosus. *Comput. Mechanics*, 2004, **34**(2), 147–163.

38 **Oxland, T. R.** and **Lund, T.** Biomechanics of stand-alone cages and cages in combination with posterior fixation: a literature review. *Eur. Spine J.*, 2000, **9**(Suppl. 1), S95–S101.

39 **Gerber, M., Crawford, N. R., Chamberlain, R. H., Fifield, M. S., LeHuec, J. C.,** and **Dickman, C. A.** Biomechanical assessment of anterior lumbar interbody fusion with an anterior lumbosacral fixation screw-plate: comparison to stand-alone anterior lumbar interbody fusion and anterior lumbar interbody fusion with pedicle screws in an unstable human cadaver model. *Spine*, 2006, **31**(7), 762–768.

40 **Panjabi, M. M., Henderson, G., Abjornson, C.,** and **Yue, J.** Multidirectional testing of one- and two-level ProDisc-L versus simulated fusions. *Spine*, 2007, **32**(12), 1311–1319.

41 **Panjabi, M. M., Malcolmson, G., Teng, E., Tominaga, Y., Henderson, G.,** and **Serhan, H.** Hybrid testing of lumbar Charite discs versus fusions. *Spine*, 2007, **32**(9), 959–966.

42 **Etebar, S.** and **Cahill, D. W.** Risk fractures for adjacent segment failure following lumbar fixation with rigid instrumentation for degenerative instability. *J. Neurosurg.*, 1999, **90**(Suppl. 2), 163–169.

43 **Aota, Y., Kumano, K.,** and **Hirabayashi, S.** Post-fusion instability at the adjacent segments after rigid pedicle screw fixation for degenerative lumbar spinal disorders. *J. Spinal Disorders*, 1995, **8**(6), 464–473.

44 **Rohlmann, A., Zander, T., Bock, B.,** and **Bergmann, G.** Effect of position and height of a mobile core type artificial disc on the biomechanical behaviour of the lumbar spine. *Proc. IMechE, Part H: J. Engineering in Medicine*, 2008, **222**(2), 229–239.

45 **Zhong, Z. C., Chen, S. H., Chen, W. J.,** and **Hung, C.** Comparison of the load and displacement controlled finite element analyses on fusion and non-fusion spinal implants. *J. Biomechanics*, 2007, **40**(S2), S353.

46 Nachemson, A. Lumbar intradiscal pressure. In *The lumbar spine and back pain* (Ed. M. I. V. Jayson), 1987, pp. 191–203 (Churchill Livingstone, Edinburgh).

47 Qunit, U., Wilke, H. J., ShiraziAdl, A., Parnianpour, M., Löer, F., and **Claes, L. E.** Importance of the intersegmental trunk muscles for the stability of the lumbar spine. A biomechanical study *in vitro*. *Spine*, 1998, **23**(18), 1937–1945.

48 Patwardhan, A. G., Havey, R. M., Meade, K. P., Lee, B., and **Dunlap, B.** A follower load increases the load-carrying capacity of the lumbar spine in compression. *Spine*, 1999, **24**(10), 1003–1009.